

Emergence of spatial structure from causal sets

D Rideout¹ and P Wallden²

¹ Perimeter Institute for Theoretical Physics, 31 Caroline St N, Waterloo, ON N2K 1S5, Canada

² Raman Research Institute, Sadashivanagar, Bangalore - 560 080, India

E-mail: ¹ drideout@perimeterinstitute.ca, ² petros@rri.res.in

Abstract. There are numerous indications that a discrete substratum underlies continuum spacetime. Any fundamentally discrete approach to quantum gravity must provide some prescription for how continuum properties emerge from the underlying discreteness. The causal set approach, in which the fundamental relation is based upon causality, finds it easy to reproduce timelike distances, but has a more difficult time with spatial distance, due to the unique combination of Lorentz invariance and discreteness within that approach. We describe a method to deduce spatial distances from a causal set. In addition, we sketch how one might use an important ingredient in deducing spatial distance, the ‘ n -link’, to deduce whether a given causal set is likely to faithfully embed into a continuum spacetime.

1. Introduction

1.1. Fundamental Discreteness

There are many reasons to believe that some sort of Planck scale discreteness will be present in any theory of quantum gravity. Perhaps the most convincing evidence is the finiteness of black hole entropy, which requires a cutoff at around the Planck scale. Thus we expect quantum gravity to be described as a discrete theory of geometry, in some form or other. One can regard the continuum as *emerging* from the discrete, in a similar way in which continuum theories for fluids emerge from the underlying physics of their discrete molecules.

In the case of fluids, the discrete elements (molecules) naturally live in a continuum background, and inherit their interrelationships from their embedding in this background. The situation for gravity, however, is different. There it is natural to expect that the discrete elements do not live in a background medium. In order to recover geometry, in this absence of a background, one must impose some sort of relationship among the discrete elements, for example in the form of a graph or binary relation, which indicates which discrete elements are ‘nearest neighbors’ in spacetime.

It is important to note in this vein that nature appears to satisfy local Lorentz invariance, at least to the degree accessible by current observations. Since the intuitive notion of nearest neighbors is naively frame dependent, a fundamental relation for discrete spacetime must contain the nearest neighbors for every Lorentz frame. Thus one expects that the number of nearest neighbors of any element will be infinite (or if finite they should generically extend to cosmological scales). From these heuristic arguments one may expect that the discreteness of quantum gravity may be expressible, in its simplest form, as some sort of very highly connected graph or binary relation.

As suggested above, it makes sense to guess that a fundamental relation for discrete quantum gravity would be compatible with the Lorentz symmetry. Stated the other way around, one might expect that the fundamental relation is such that it allows the macroscopic Lorentz symmetry to emerge naturally from the discrete. There are two possibilities which come to mind, one which takes a microscopic causal ordering as this relation, and another which takes spatial nearest neighbors, as given by the invariant spacetime interval ds^2 . It is not possible to specify both freely because the causal relation alone is sufficient to recover the metric up to a conformal factor. Thus given one relation, it must be possible to deduce the other.

A number of approaches to quantum gravity take the second approach, such as loop quantum gravity¹ [1–3], ‘quantum graphity’ [4], and the approach outlined in [5]. Quantum graphity, for example, has as its fundamental discrete structure a graph which is regarded as a spatial object, which evolves in time. It postulates a form for the Hamiltonian which describes its time evolution, and from this one is able to derive the presence of light cones and non-trivial causal structure [5, 6].

Here we take the alternate approach, that microscopic causal ordering is fundamental, and show that it is possible to derive from it a symmetric, spacelike relation, at least for discrete structures (causal sets) which are well approximated by Minkowski space. This approach has the advantage that one can address the question of how continuum structures emerge from the discrete, without reference to a particular dynamical law.

The ability to recognize continuum properties from the discrete relation may be an important stepping stone toward constructing a full theory of quantum gravity. In particular, most of our understanding of how to formulate gravitational dynamics is within the continuum. It would be helpful to understand how this carries over to the discrete context. This understanding may also provide crucial hints as to a fundamental origin of black hole entropy and the covariant entropy bound, by providing clues as to how to count states associated with a spacelike or null hypersurface [7].

Once we have the ability to deduce spatial distances between discrete elements in the approximating continuum, it is not difficult to use this to compose a symmetric, spatial nearest neighbor relation, which can be useful for recovering topology and geometry of curved spacetime. In addition this may allow contact with other approaches to quantum gravity, which hold the spacelike relation to be fundamental.

We address the question of how to deduce the spatial distances in an approximating continuum, given only a discrete partial order. It turns out that, while the recovery of timelike distances from the discrete causal ordering is relatively straightforward, recovering spacelike distances is much more difficult, due to the relatively unfamiliar nature of Lorentz invariant discreteness.

1.2. Causal Sets

The causal set approach to quantum gravity is based on two observations. One is that the causal structure of a spacetime, namely a list of which events ‘can causally influence’ which others, is a very rich structure, enough to reconstruct the conformal metric. The other is the abundance of evidence suggesting that some sort of discrete structure underlies continuum spacetime. [8]

The intent is to approach ‘quantization’ via histories, i.e. to take the *histories*, rather than states defined on some ‘spatial hypersurface’, as the fundamental objects of the theory. The quantum theory can then be expressed in terms of some appropriate generalization of the Feynman path integral [9–11].

¹ Loop quantum gravity does not literally take this approach, however the fundamental object with which the theory is expressed is purely spatial in character, and the edges of the spin network encode (among other things) a binary spatial relation on the vertices.

In the causal sets approach, the histories are taken to be *causal sets*, which are countable sets of ‘atoms of spacetime’, endowed with a partial order relation \prec which is transitive and irreflexive. For a causal set C , transitivity requires that if $x \prec y$ and $y \prec z$ then $x \prec z$, $\forall x, y, z \in C$. Irreflexivity is simply the condition that no element can precede itself, namely $x \not\prec x \forall x \in C$. To enforce discreteness, one imposes a local finiteness condition, that every *order interval* $[x, y] = \{z \in C | x \prec z \prec y\}$ has finite cardinality.

The correspondence between the discrete causal set and a continuum spacetime is described in terms of a *faithful embedding*, which is an order preserving map ϕ from a causal set C to a spacetime (M, g) , which has the property that “the number of elements mapped into any region of spacetime volume V is Poisson distributed with mean V ”. Here *order preserving* means that two events $\phi(x)$ and $\phi(y)$ in the image of ϕ are causally related in the spacetime ($\phi(x) \in J^-(\phi(y))$) iff the corresponding elements in C are related $x \prec y$. The Poisson distribution with mean V assigns a probability of $\frac{V^n e^{-V}}{n!}$ to the event of mapping n elements to the region of volume V .

A faithful embedding is easy to realize, one simply selects points in the target spacetime (M, g) at random by a Poisson process (a ‘sprinkling’), and then computes a partial order on them using the causal structure of the spacetime. This gives a causal set C , along with a faithful embedding ϕ of C into (M, g) . It is useful to make use of the map ϕ implicitly when discussing the causal set, so that one can speak of “the causet elements in a region of, or at points in, (M, g) ” to refer to those elements which are mapped to regions of (M, g) by ϕ .

It is important to keep in mind, however, that it is the discrete causal set that is fundamental, and the continuum into which it may faithfully embed is to be regarded only as an approximation to the discrete substructure. The faithful embedding is merely a tool with which to discuss how the continuum arises from the discrete. It is worth remarking that it may be the case that a ‘physical’ causal set may only faithfully embed into a continuum spacetime after some coarse graining, so the physics near the Planck scale need not be continuum-like.

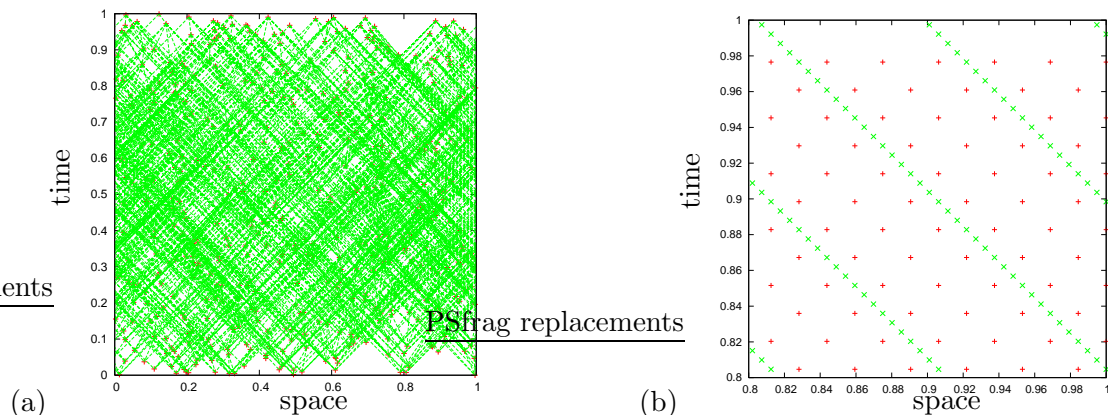


Figure 1. Two embeddings of a causal set into a spacetime. (a) The causal set has 512 elements, and is faithfully embedded into a flat $2d$ spacetime with cylindrical topology $S^1 \times I$. The links are shown in green. (b) The figure depicts a (non-faithful) embedding into a region of $2d$ Minkowski space. The red and green distributions of points are related to each other by a boost of $4/5$.

Figure 1 illustrates two embeddings of causal sets into spacetimes, one faithful and one not. Some important features to note in these diagrams regard the behavior of the *links* in the causal sets, which are those relations which are ‘irreducible’, in that they are not implied by transitivity. For the faithful embedding on the left, one can note that (a) the number of links connected to

each element is very large, and (b) the vast majority of links connect elements from very distant regions of the spacetime, in any given frame (such as that of the figure). This is because any given link only appears short in one frame, it will be long in all others. Since almost all frames are ‘another frame’, almost all links appear to be very long. In the embedding on the right, on the other hand (in which the links are not shown explicitly), each element is connected to only four links. In the red frame the links connect nearby elements, while in the green frame the ends of the link are becoming more distant in one direction (and extremely close in the other). This embedding fails the ‘faithfulness’ condition, that the expected number of elements mapped to any region is equal to its volume. There are obviously very large regularly shaped regions which fail this criterion. In this way regular lattices fail to be manifoldlike, if one does not go all the way to the continuum ($\rho \rightarrow \infty$) limit. Thus in this way the Lorentz invariance appears to in fact *emerge* from a discrete relational theory, as the only way in which the correspondence between number of discrete elements and spacetime volume can be independent of the region one is considering.

1.3. Hauptvermutung

Named after the famous conjecture in topology, that every triangulable space has a unique triangulation (which was later proved to be false), it is conjectured that a causal set which faithfully embeds into a spacetime manifold determines the manifold up to ‘approximate isomorphism’. Somewhat more precisely, we can define the ‘Hauptvermutung’ (central conjecture) for causal sets as follows (see figure 2). Given a causal set C , and two faithful

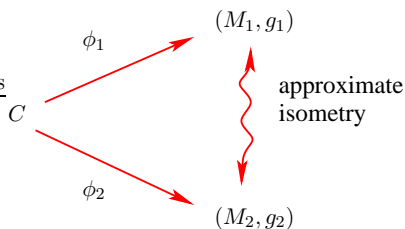


Figure 2. ‘Hauptvermutung’ of causal sets

embeddings $\phi_1 : C \rightarrow (M_1, g_1)$ and $\phi_2 : C \rightarrow (M_2, g_2)$ from C into spacetime manifolds, then (M_1, g_1) and (M_2, g_2) must be approximately isometric. The ‘approximately’ is necessary because of the discreteness — the embedding is obviously blind to continuum structures smaller than the discreteness scale. The precise mathematical statement of the Hauptvermutung remains open, however there does exist a body of work on defining a distance measure between Lorentzian geometries [12].

It may seem a lot to hope, to recover the full spacetime geometry from the discrete order. However, the expectation is not unreasonable. The microscopic order more-or-less directly encodes the macroscopic causal order. By a theorem of David Malament and others [13, 14], we know that the causal ordering of events in spacetime contains enough information to recover the topology, differential structure, and conformal metric. Thus all that remains is the conformal factor, which encodes volume information. Here the discreteness plays a crucial role, by providing the missing volume information, via the correspondence between number and spacetime volume expressed in the faithfulness condition on the embedding. In the continuum one needs to add the gravitational field to get geometry, while in the discrete the geometry arises naturally, without needing to add any additional mathematical structures. Thus it is not unreasonable to expect that one can recover the complete spacetime geometry from the discrete causal order. Note that the Lorentzian signature arises naturally, as the only one capable of distinguishing past from future.

1.3.1. Dimension An obvious question which arises when discussing causal sets is how can one predict the dimension of an approximating spacetime, given only the causal set. There have been a number of proposals for how to do this, for example the midpoint scaling and Myrheim-Meyer dimension, which are both described in [15, 16]. The Myrheim-Meyer dimension [17, 18] works by counting the number of relations in an order interval, and comparing it with what one would get from sprinkling into \mathbb{M}^d .

In section 7 we sketch an alternate method for estimating the dimension of causal sets, based upon the counting of n -links (defined in section 4), and present some preliminary results.

1.3.2. Timelike distance Since the fundamental relation defining the causal set is intrinsically timelike, one can imagine that it is relatively straightforward to extract timelike distances from the causal set. The natural choice which is likely extendable to curved spacetime is to count the number of links in the longest chain connecting the two related elements $x \prec y$ [17, 19, 20]. (In general such a longest chain will be far from unique. Figure 3 shows the collection of longest chains between a pair of elements in \mathbb{M}^2 .)

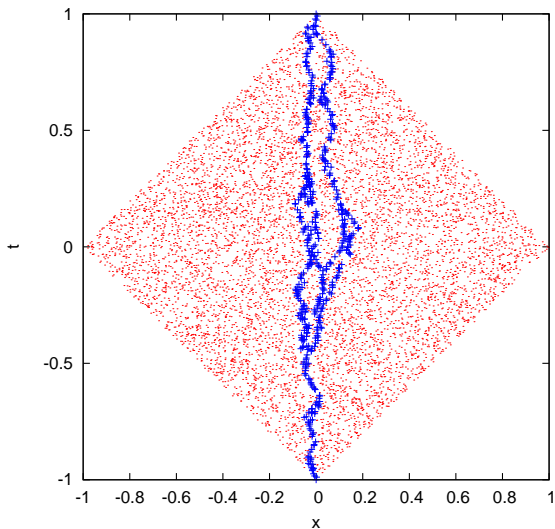


Figure 3. The collection of longest chains (*geodesics*) between a pair of elements in \mathbb{M}^2 .

By a theorem stated in [21], we know that this length L converges to the proper time separation between x and y , in particular

$$\frac{L}{(\rho V)^{1/d}} \rightarrow m_d$$

in probability as $\rho V \rightarrow \infty$. Here ρ is the sprinkling density, V is the volume of the interval $[x, y] = J^+(x) \cap J^-(y)$, d is the spacetime dimension, and m_d is a constant depending only on the dimension. It's exact value is known only in two dimensions, $m_2 = 2$. It's value in three dimensions was measured in [22] to be $m_3 = 2.296 \pm .012$. If we write the volume of the interval as $V = D_d T^d$, with T the proper time we seek, and D_d a dimension dependent coefficient (we will need $D_3 = \frac{\pi}{12}$), then in the infinite ρ limit

$$T = \frac{L}{m_d \rho^{1/d} D_d^{1/d}}. \quad (1)$$

To get some feel for how well this works 'in practice', we check it on a computer, using code for the Cactus high performance computing framework [23] mentioned in [22]. We sprinkle into

an interval of height $T = 2$ (in arbitrary units), count the length of the longest chain within that interval, and from it compute, from (1), an ‘effective’ m_d

$$m_d^{\text{eff}} = \frac{L}{T(\rho D_d)^{1/d}} \quad (2)$$

which is relevant for finite ρV . For $d = 3$ we get the results depicted in figure 4. Each datapoint

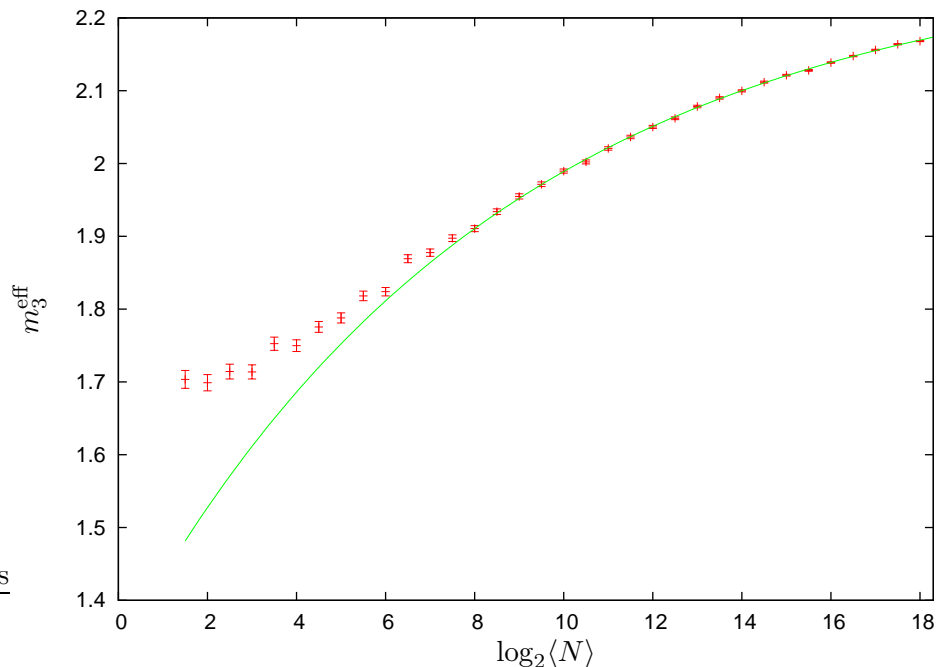


Figure 4. Convergence of length of longest chain L to proper time T for a faithful embedding into an interval of \mathbb{M}^3 . The green fit to the asymptotic form measures the constant of proportionality m_3 .

results from 1600 sprinklings into an interval of \mathbb{M}^3 , each with a mean number of elements $\langle N \rangle$ (the mean of the Poisson distribution) as indicated. We plot the mean m_3^{eff} from (2), along with the standard estimate of its error. The fit is to the function $m_3 + ae^{b \log_2 \langle N \rangle}$, for the datapoints $\langle N \rangle \geq 2^8$. We get $m_3 = 2.2856 \pm 0.0063$, which is consistent with the measurement in [22] (that employs a slightly different procedure)².

Note that for any finite region (ρV finite), the m_3^{eff} is less than the asymptotic value m_3 , and thus a measurement of proper time using the length of the longest chain via (1) will always underestimate the continuum proper time. We call this effect *timelike underestimation*.

2. Early Prescription for Spacelike Distance

We would like to recover the full spacetime geometry from the discrete causal ordering. We have seen above how to get dimension and timelike distances. How can one extract spatial

² Here we are effectively conditioning on the existence of sprinkled elements at the endpoints of the interval. Since the occupation probability at each point in a Poisson process is independent of those at every other point, this should make no difference. In [22] the authors select a pair of elements that land nearest the endpoints of the interval, and use the interval formed by those two elements. It appears that this distinction does not affect our measurement of m_3 .

information? How does spatial geometry come out? We start with the simple question of spatial distance in flat spacetime. Can we recognize the spatial distance between elements of a causal set which can be faithfully embedded into Minkowski space?

An obvious first guess is to use the spacelike points to locate a timelike pair, whose distance is the same as the spacelike distance, and then use the timelike method above. In the continuum, this can be done, as follows. Consider a pair of spacelike separated elements x and y , whose spatial distance we would like to measure. Consider those pairs of points w in the common past $J^-(x) \cap J^-(y)$ and z in the common future $J^+(x) \cap J^+(y)$ which minimize the timelike distance (length of the longest chain L_{wz}) between w and z . In the continuum, every such pair is separated by exactly the spacelike distance between x and y .

In the discrete causal set context, the above construction works fine for causal sets which faithfully embed into \mathbb{M}^d , for $d < 3$. This is because for $d = 2$ there is a unique choice for the pair (w, z) in the continuum (w is the point at the intersection of the past light cones of x and y , and z is the intersection of their future light cones). For a causal set sprinkled into \mathbb{M}^2 , the pairs (w, z) at minimum timelike separation (length of the longest chain) will lie close to the corresponding ‘minimizing pair’ in the continuum.

At larger dimension d , in the continuum, one finds a $d - 2$ dimensional submanifold of points (w, z) at minimum timelike separation. One way to see this is that the pair (x, y) breaks the Lorentz symmetry in one direction, but the picture is still invariant under boosts in any orthogonal direction. Starting from any arbitrary frame, in which the pair (w, z) both occur at the centroid of x and y , one can trace out the submanifold by applying all boosts which leave x and y invariant.

Unfortunately this infinity of ‘minimizing pairs’ causes problems in the discrete case of a random sprinkling, because it causes one to consider an infinite number of independent regions when computing the spatial distance between x and y . To understand why this simple prescription for spacelike distance fails in dimensions greater than 1+1, consider the spacelike pair (x, y) in figure 5(a). Shown are a pair (w, z) (a *minimizing pair*) which are close to the intersection of x and y ’s future and past light cones, and might locally minimize the length of the longest chain between w and z . However, our distance prescription seeks a global minimum, not a local minimum, so we must consider ‘what happens in other frames’ as well. Figure 5(b) depicts the same situation, in the frame in which x and y are simultaneous, and w and z occur at the same spatial location. (x and y are not shown explicitly in the diagram; they are displaced into and out of the page by a small amount.) Shown are three candidates for pairs (w, z) , along with the order interval between them, which is the portion of the causal set which determines the length of the longest chain between them. If we compare the intervals for two pairs which are ‘highly boosted with respect to each other’ (meaning the boost parameter relating the frames in which the pairs (w, z) are simultaneous) have very little overlap. But each of these intervals contains the same spacetime volume of Minkowski space. The sprinklings in each of these regions is independent (save the tiny region of overlap), since the Poisson distribution is independent at each point. Since there are an infinite number of candidate pairs (w, z) , to find the global minimum, we must sample the Poisson distribution an infinite number of times, to get the portion of the causal set in each of these independent regions. One possible result for this sample, which has finite probability, is that the region is empty. Thus this event (of finding a candidate pair (w, z) whose interval $[w, z]$ is empty of sprinkled elements) must occur an infinite number of times, and so the distance between x and y will always be exactly two³, regardless of where they fall in Minkowski space.

³ two because by definition $w \prec x \prec z$ and $w \prec y \prec z$ (and $x \not\prec y$), each of which are chains of length 2.

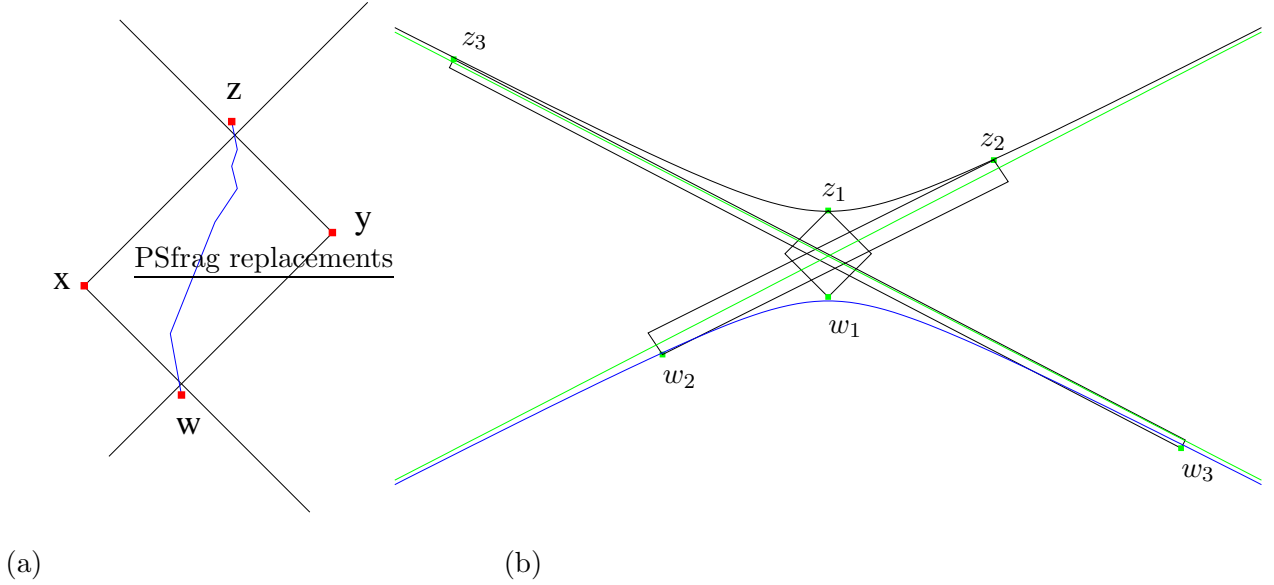


Figure 5. (a) Two spacelike elements x, y in \mathbb{M}^3 , and a pair w, z in their common past/future. (b) The elements x and y lie at the center of the figure, but displaced out of and into the page by some finite equal amount. The hyperbolae indicate the intersection of the past and future light cones of x and y . The long straight green lines are the asymptotes of the hyperbolae. The green dots with black intervals indicate the projection of the causal intervals for minimizing pairs onto the plane of the page.

2.1. Numerical evidence

The above argument depends upon a sprinkling into the entirety of Minkowski space. What if one has a sprinkling into a finite region of Minkowski, such as might be physically realistic in a finite universe, or as can be simulated on a computer? Is it possible to see the above degeneracy in spatial distance, while considering only that portion of the causal set which is contained in a finite portion of Minkowski space? The probability to see a region of spacetime volume V which is empty of sprinkled elements is e^{-V} . In \mathbb{M}^3 , an interval of height $T = 4$ has volume $V = \frac{\pi}{12}4^3 \approx 16.755$, and the probability to find an empty interval of height $T = 4$ is 5×10^{-8} . Thus a lower bound on the size of a region of \mathbb{M}^3 which would be required to see this degenerate distance is $17/5 \times 10^{-8} \approx 3 \times 10^8$.

To explore this on the computer, we sprinkle into a $T \times T \times \Delta$ box, as illustrated in figure 2.1. In this section we use units such that $\rho \equiv 1$. The spacelike pair (x, y) are placed at the small red squares, which lie in the center of the two largest faces as shown. In the simulations, we hold the distance Δ between x and y fixed, while increasing the size of the box in the lateral directions. If the distance measure works well, then obviously increasing the size of the box in the lateral directions should have no affect. We see in figure 2.1 that this is not the case. There we show the results from two simulations, one with $\Delta = 4$, and one for a more distant pair $\Delta = 8$. X is the smallest value of (1) for a pair of elements (w, z) in the common past and future of x and y . In all these simulations we use a $m_3^{\text{eff}} = 1.75815$, which we carefully measure to be the appropriate value for an interval of size $\rho V = \frac{\pi}{12}4^3$. This eliminates the effect of timelike underestimation.

At $T = \Delta$ the common future and past of (x, y) are outside of the sprinkling region, so the spatial distance is undefined. For slightly larger T , we observe a substantial overestimation of the continuum distance Δ . This occurs because it is unlikely that a sprinkled element will land close to the intersection of x and y 's light cones. The pair (w, z) will always be separated by a continuum (timelike) distance $> \Delta$, hence the overestimation. This overestimation will always

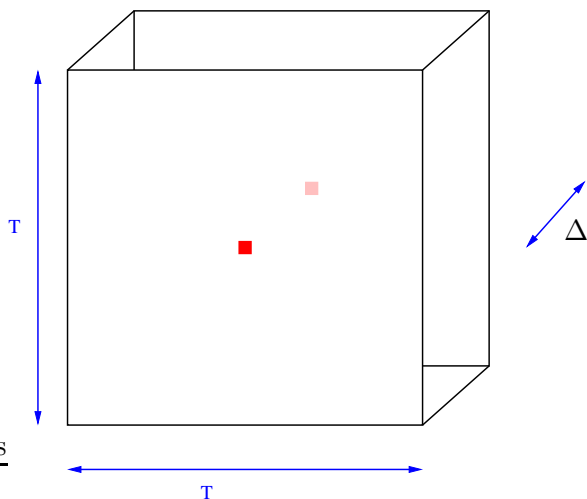


Figure 6. Growing region of M^3 into which we sprinkle. Δ is held fixed to a small value (4 or 8), while T is increased as far as the computer allows ($2^{7.75} \approx 215$).

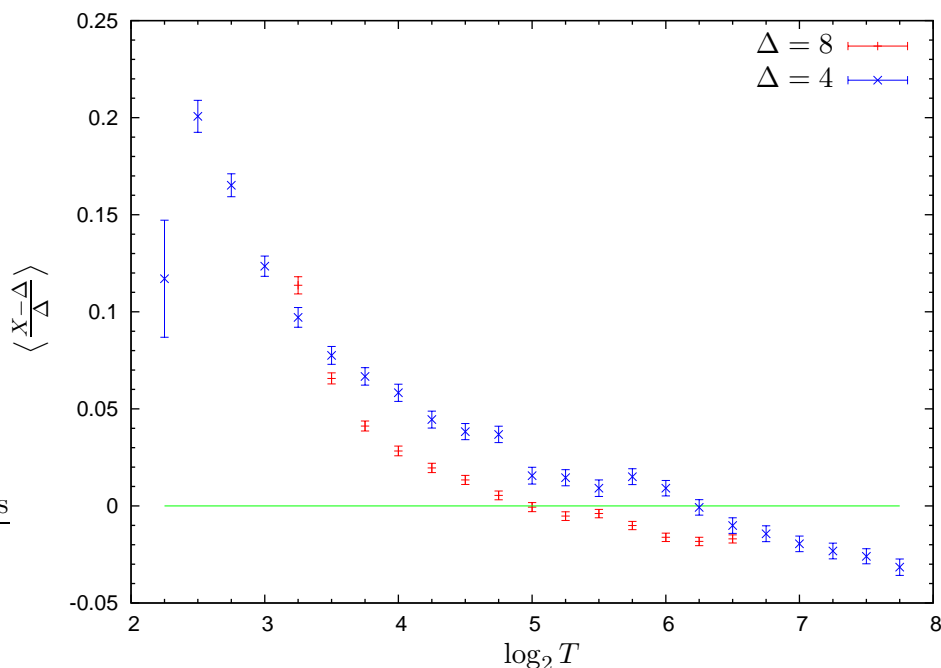


Figure 7. Demonstration of the degeneracy of the ‘naive’ prescription for spacelike distance of section 2. Each data point gives the mean and standard error for 900 sprinklings.

be of the order of the discreteness scale, and so, even though in this context is rather large, will be irrelevant for macroscopic distances.

At large T , we see the overestimation decrease, past zero to negative values. Since the use of m_3^{eff} already corrects for the timelike underestimation effect, this decrease must be due to the degeneracy of the spacelike distance definition of section 2. If we could expand T all the way to infinity, we expect to see the deviation decrease to $\frac{D_3^{1/3} m_3^{\text{eff}}}{\Delta}^{-\Delta} \approx -.55544$ for $\Delta = 4$.

It appears that this naive prescription for spatial distance on a causal set fails, due to the Lorentz invariant nature of the embedding, and the random nature of the Poisson process. How might one deduce spatial distances on a causal set? One possibility is to select enough additional elements to eliminate the boost freedom mentioned above. This leads to more of a ‘diameter’

measure, than a distance measure, in that it can be interpreted as giving the diameters of spheres defined by the d elements. This is described in section 3.

An alternate proposal is to take advantage of the fact that links in a causal set closely track the light cones, and this can be used to locate appropriate pairs (w, z) without resorting to a global minimum. This leads to the 2-link distance proposal of section 5.

3. Diameter measures

In order to locate a relatively unique pair (w, z) , one can select, instead of simply a pair of elements (x, y) , a collection of d mutually unrelated elements (an *antichain*) in \mathbb{M}^d . One can then select a w which is in the common past of the entire antichain, and a z which is in the common future, and seek a pair which minimizes the length of the longest chain between w and z . It turns out that this measures the diameter of the smallest $d - 1$ -ball, which lives on the surface of simultaneity of all d elements of the antichain, and contains them all. It is called l_g in [22].

Using the same antichain, one can also construct a $d - 2$ -sphere, which lives on the same spatial hypersurface, and contains each of the d elements of the antichain. It is possible to write down an expression in terms of order invariants which measures the diameter of this sphere. It is called l_s in [22]. Both of these diameter measures are described there in detail, along with a number of possible applications.

4. n-links

As mentioned above, an alternate approach to measuring spatial distances in a causal set is to use the fact that the *links* of the causal set lie very close to the light cone in a faithful embedding, and effectively give the light cone structure of the causet. One way to see this is that the proper time between a pair of related elements is measured by the length of the longest chain connecting them. A null relation corresponds to a minimum proper time (zero), so the analogue in a causal set should correspond to a minimum length of the longest chain, which is a single link. Figure 8 depicts some of the links to the future of an element in Minkowski space.

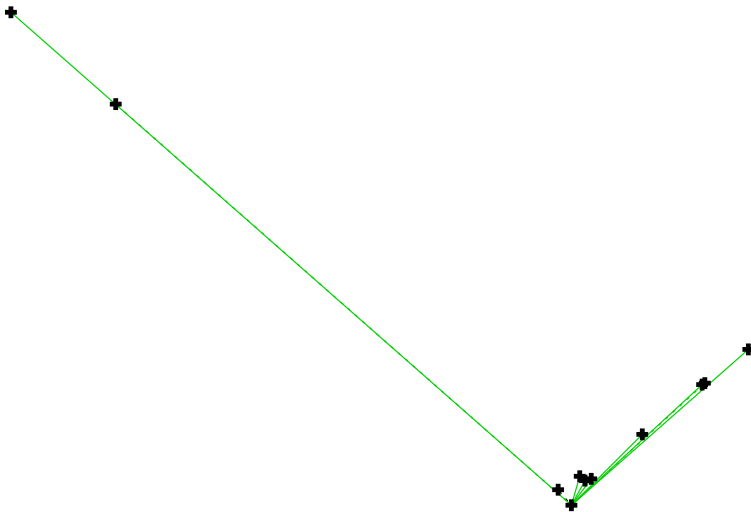


Figure 8. Links to the future of an element in Minkowski space.

We define an n -link as an element which is linked to each member of an n element antichain. If this element is to the future (past) it is called a future (past) n -link. Some examples are depicted in figure 9. Given the above discussion, it is fairly clear that an n -link corresponds to the intersection of light cones emanating from each element of the antichain.

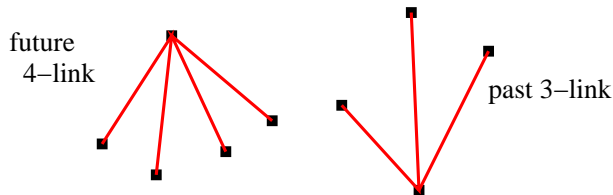


Figure 9. Illustration of n -links.

How many n -links does one expect to find, to the future of a given n -antichain (an antichain with n elements), for a causal set faithfully embedded into \mathbb{M}^d ? For $n < d$, one expects an infinite number, for similar reasons as discussed in section 2. Roughly speaking n elements are not enough to select a surface of simultaneity, so in each of an infinite number of frames one expects to see an n -link with some finite probability. For $n > d$ there should not be any n -links, unless the n elements are arranged in some special way (e.g. as in figure 8, which depicts a 9-link within a sprinkling of \mathbb{M}^2). For $n = d$, the intersection of the future light cones consists of a single point. The probability that there is an element near (and to the future of) this point is moderate, but the probability that it is linked to each element of the antichain diminishes rapidly with their distance.

One application of n -links in causal sets is they can provide a definition of spatial distance which is devoid of the degeneracy from which the definition given in section 2 suffers. This will be explained in detail in the next section.

Another application may be that they can be used as an indicator of ‘manifoldlikeness’ in a causal set (cf. [24]). The behavior of the number of n -links in a causal set that is well approximated by Minkowski space is sketched above, which is potentially quite specific given that it should hold for all n . For example, if one does have a causal set which faithfully embeds into \mathbb{M}^d , then the above behavior should fairly clearly pick out the value of d . This could be compared with other dimension estimators as a further test. An initial attempt at identifying manifoldlikeness in this way appears in section 7 below.

5. 2-link Distance

The definition of spacelike distance given in section 2 fails because for any spacelike pair (x, y) there are an infinite number of potential ‘minimizing pairs’ (w, z) which lie close to the intersections of the light cones of x and y . Since one takes a global minimum over all such pairs (w, z) , one gets a trivial result. If one could take an average of ‘minimizing pairs’ (w, z) , rather than minimum, this problem could be avoided. The problem is how to locate appropriate pairs of elements close to the intersection of the light cones of x and y , however this is exactly what is provided by 2-links.

We thus define the 2-link distance between two unrelated elements x and y by the following algorithm:

- (i) Compute the set of all future 2-links of x and y .
- (ii) For each future 2-link z , compute the smallest distance L_i from an element $w \in \text{past}(x) \cap \text{past}(y)$ to z .
- (iii) Store L_i .
- (iv) Repeat the above with ‘future’ and ‘past’ interchanged.
- (v) Compute the average of the L_i .

In figure 10 we contrast 2-link distance against the ‘naive’ spatial distance of section 2. Each data point gives the mean and its error, for 900 sprinklings into the boxes of figure 2.1. Again we see the large spacelike overestimation for the 2-links, as for the naive spatial distance. As

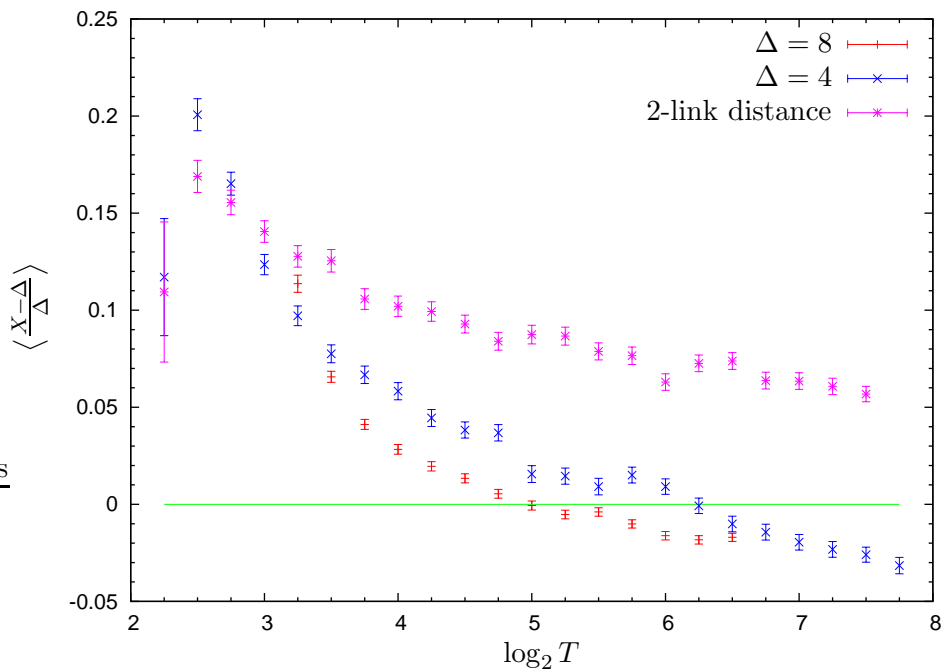


Figure 10. Comparison of 2-link distance at $\Delta = 4$ (magenta) with the ‘naive’ prescription for spacelike distance of section 2 (red and blue).

the size of the box is increased, its accuracy increases slightly because it finds more 2-links with which to estimate the distance. The random fluctuations in this figure are smaller than those of figure 14 of [22] because here we include past 2-links as well as future, and also condition on there being causet elements at the center of the faces of the box.

One may wonder how common are 2-links, if we are to rely on their existence in order to define spatial distance in a finite region. We expect to find an infinite number in dimensions > 2 , but this assumes infinite Minkowski space. Will there exist many in a reasonably sized portion of our universe? We address this question by searching for 2-links, using the same computation as described in section 2.1, with $\Delta = 8$. In this case, however, we simply count the number of (future and past) 2-links, rather than compute the 2-link distance itself. The results are shown in figure 11. The error bars indicate the usual estimate of the standard deviation. Given that they overlap with, or are not far from extending to, zero, there will be a number of sprinkled causets which do not find any relevant 2-links. In these cases we simply discard the causet, though we do count it toward the total number generated (900). The blue curve is a fit to $a + b \ln \langle T \rangle$. In figure 12 we count the number of 2-links in a rectangular $T \times 8 \times T \times T$ box. The spacelike elements (x, y) are placed in the centers of the x -faces, as before. Here the number of 2-links grows linearly with the box size, as one might expect. The fitting function is $a + b \langle T \rangle$. Here we show error bars for both the standard deviation and the error in the mean.

6. Spatial nearest neighbors and curved spacetime

One can use the 2-link distance in the context of curved spacetime, however it has the unfortunate property that the distance between x and y depends upon portions of the causal set which are arbitrarily ‘distant’ from x and y . To measure a length in my lab I must in principle consider the happenings in Andromeda millions of years ago and also millions of years from now. Given that we know that spacetime is locally flat, we can truncate the search for 2-links at some intermediate mesoscale, beyond which we expect curvature effects to become relevant. It may be that the introduction of a mesoscale is inevitable in discrete quantum gravity, as it arises in a number of quite different contexts [24, 25].

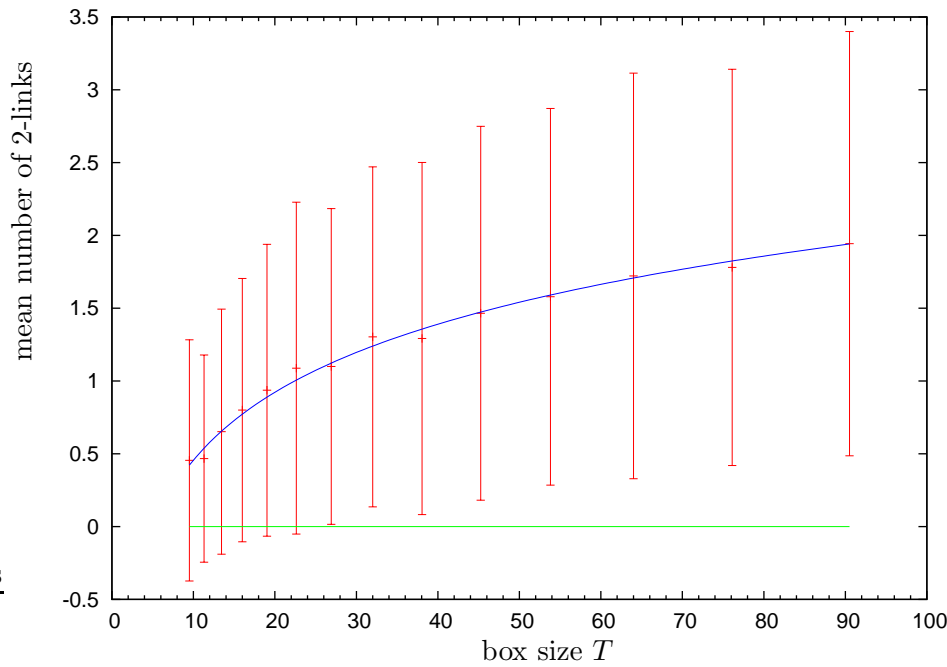


Figure 11. Expected number of 2-links in the sequence of boxes of figure 2.1. Each data point gives the mean and standard deviation from 900 sprinklings.

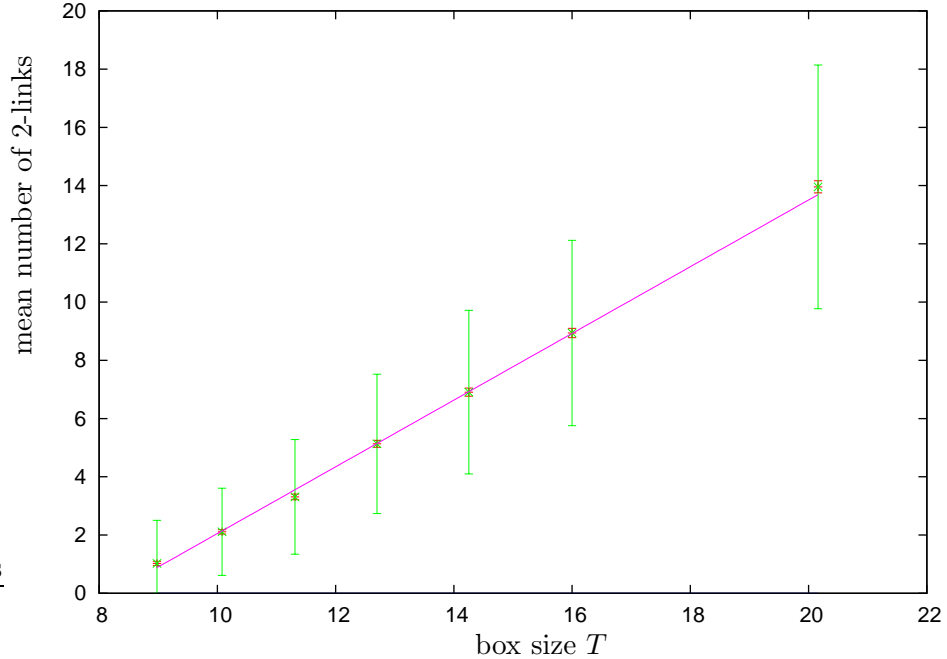


Figure 12. Expected number of 2-links in a sequence of boxes similar to figure 2.1, but with an added spatial dimension of size T . Here each data point gives the mean, standard deviation, and standard error, from 403 sprinklings.

In order to get a reasonable distance measure from the 2-link distance, one simply needs to find a ‘reasonable’ number of 2-links. One can thus define an ‘infrared cutoff’ in terms of some number of 2-links. This (subset of 2-links) of course depends upon an arbitrary choice of frame, but this is not a problem, in that the resulting 2-link distance should be independent of this choice, provided that the region of the causal set that they ‘enclose’ is well approximated by flat spacetime.

A proposal to address the need for the region enclosed by the ‘2-link minimizing pairs’ to be

flat is to employ the 2-link distance to locate ‘spatial nearest neighbors’ in the causal set. These would consist of unrelated pairs of elements whose 2-link distance is beneath some threshold. If the threshold is chosen small enough, then it can be easy to find enough 2-links with a quite modest cutoff. Such nearest neighbors of an element within a sprinkling of \mathbb{M}^3 is shown in figure 13.

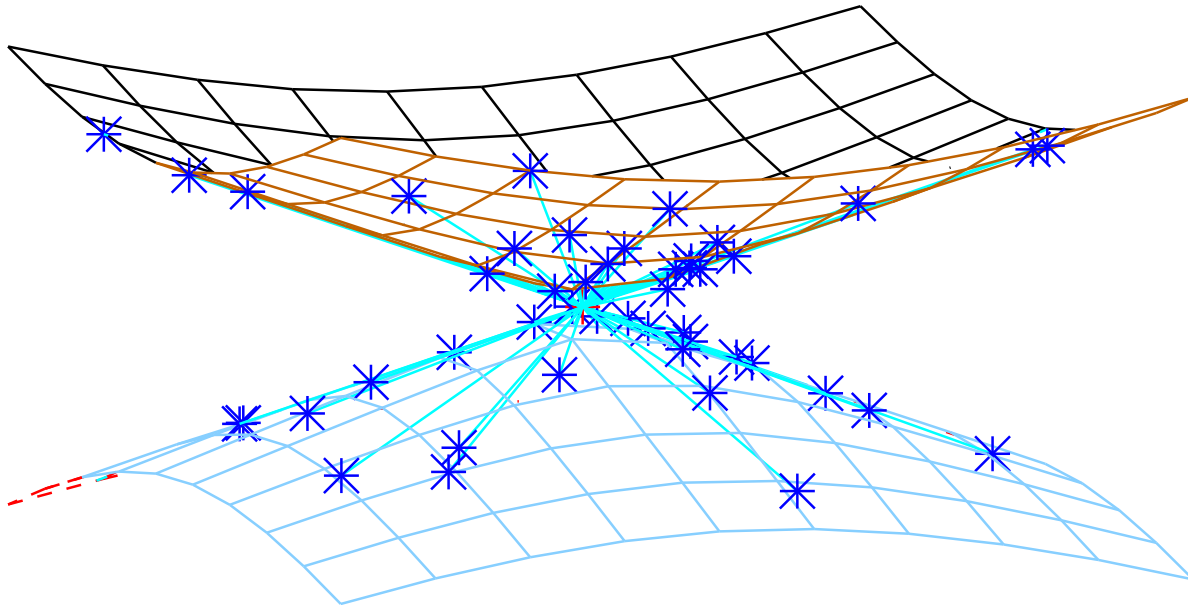


Figure 13. Spatial nearest neighbors of an element in a sprinkling into (a fixed cube in) \mathbb{M}^3 . $\langle N \rangle = 65\,536$. The future and past light cones of the ‘origin element’ x are shown. The spacelike cyan lines are drawn between x and each neighbor, for emphasis.

With such a spatial nearest neighbor relation in hand, one can define distances of curves in a curved spacetime setting. See [22] for some illustrations of spatial nearest neighbors in Minkowski space, including an adjacency graph of a spatial slice, derived from a sprinkled causal set.

7. n -links as manifoldlikeness test

It is noted in [22], and also above in section 4, that the particular behavior of the number of n -links ‘attached’ to a given antichain for sprinklings into Minkowski space may be used as an indicator for ‘manifoldlikeness’. By this we mean that, if the numbers of n -links look like what one finds for Minkowski space, with many n -links for $n < d$, few for $n = d$, and almost none for $n > d$, then the causal set may be likely to faithfully embed into \mathbb{M}^d .

To get some idea how this might work in practice, we perform a preliminary study, by counting 1- and 2-links in a number of (finite) causal sets. We find that the counts of 1- and 2-links are easily able to distinguish obviously non-manifoldlike causal sets from sprinklings, but they have difficulty distinguishing causal sets generated by the sequential growth dynamics of [26] from sprinklings into \mathbb{M}^d . Physically, one might think of an abundance of 1-links as indicating the potential existence of light cones, as one finds in spacetime, while an abundance of 2-links may indicate the existence of a spatial direction orthogonal to the pair of elements in question. 3-links could indicate spatial directions orthogonal to a plane, and so on.

The particular computation we perform is as follows. Given a causal set C , for each element x , we count the number of links l connected to x , and then form a histogram from these counts l . We do likewise for 2-links: for every 2-element antichain in C we count the number of attached

2-links, and form a histogram of these counts. For example, for the causal set in figure 14, there are six elements with 2 (1-)links (the minimal and maximal elements (those with an empty past and future respectively)), and three with 4 links (those in the middle layer). For 2-links, there are three pairs with 2 2-links (those consisting of elements in the middle layer), six with one 2-link (3 pairs each in the top and bottom layers), and six with zero 2-links (these come from pairs with elements in different layers). The corresponding histogram is displayed in figure 15.

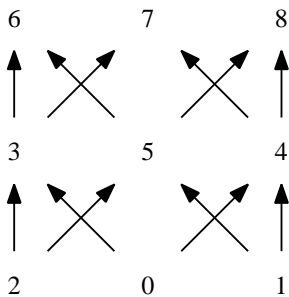


Figure 14. A tower of three 3-crowns. The numeric labels are arbitrary and have no significance.

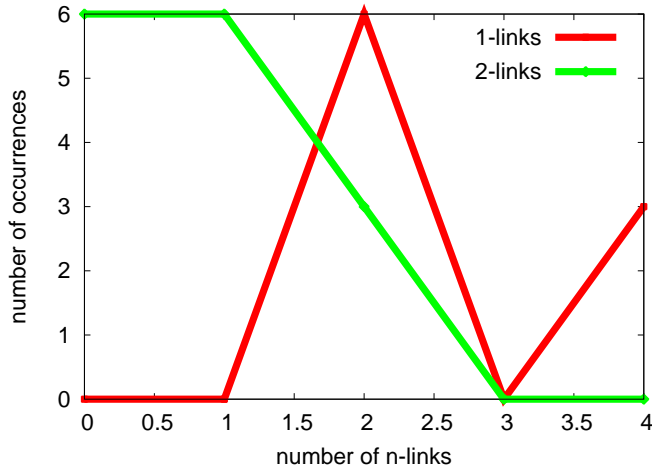


Figure 15. 1- and 2-link histograms for the causal set in figure 14. Lines are drawn between the data points for clarity.

We begin with some sprinklings into intervals of Minkowski space, to see how the counts of 1- and 2-links behave for manifoldlike causal sets. Figure 16 shows histograms of the number of links attached to a causet element, for sprinklings into six different spacetimes. Four are intervals in Minkowski space, of various dimensions. The fifth is a region of a conformally flat Friedman Robertson Walker universe, which contains the initial singularity. (The region is $\eta, x_1, x_2, x_3 \in [0, 1]$, in which coordinates the metric is $ds^2 = \eta^4(-d\eta^2 + dx_1^2 + dx_2^2 + dx_3^2)$. The spatial topology is T^3 , so $x_i = 0$ is identified with $x_i = 1$ for $i = 1 \dots 3$.) For each of these five we sprinkle with a mean number of elements $\langle N \rangle = 512$. The sixth is a $4d$ Schwarzschild black hole, where we have used the technique described in [27] to deduce the causal relations. We sprinkle $\langle N \rangle = 256$ elements into the region $0 < t < 10, 0 < r < 3M$ in Eddington-Finkelstein coordinates. Figure 14 depicts a similar histogram, for 2-links. We expect to find an infinite number of 2-links for every 2-antichain, for spacetime dimension > 2 . This manifests itself in extremely long (power law) tails, in our finite simulations. Even in two dimensions we find some 2-antichains with a large number of 2-links, though the fall off is much sharper. The fact that the results for the $4d$ Schwarzschild spacetime more closely resemble lower dimensional spacetimes may be because many of the elements get sprinkled behind the horizon, where the light cones rapidly fall into the singularity, before they have a chance to build up a large number of links.

A popular concept in physics is that we live in some sort of a product manifold, perhaps with compactified internal dimensions, such as in Kaluza-Klein or String theory, or with large extra dimensions of a braneworld scenario. To investigate how some of these ideas might play out in the causal set context, we consider sprinklings into a flat spacetime with topology $T^3 \times I$ (i.e. a box shaped region of \mathbb{M}^3 with opposite sides identified), in which we vary the size of the dimensions of the torus. Our results are given in figure 18. We see that for the case in which all

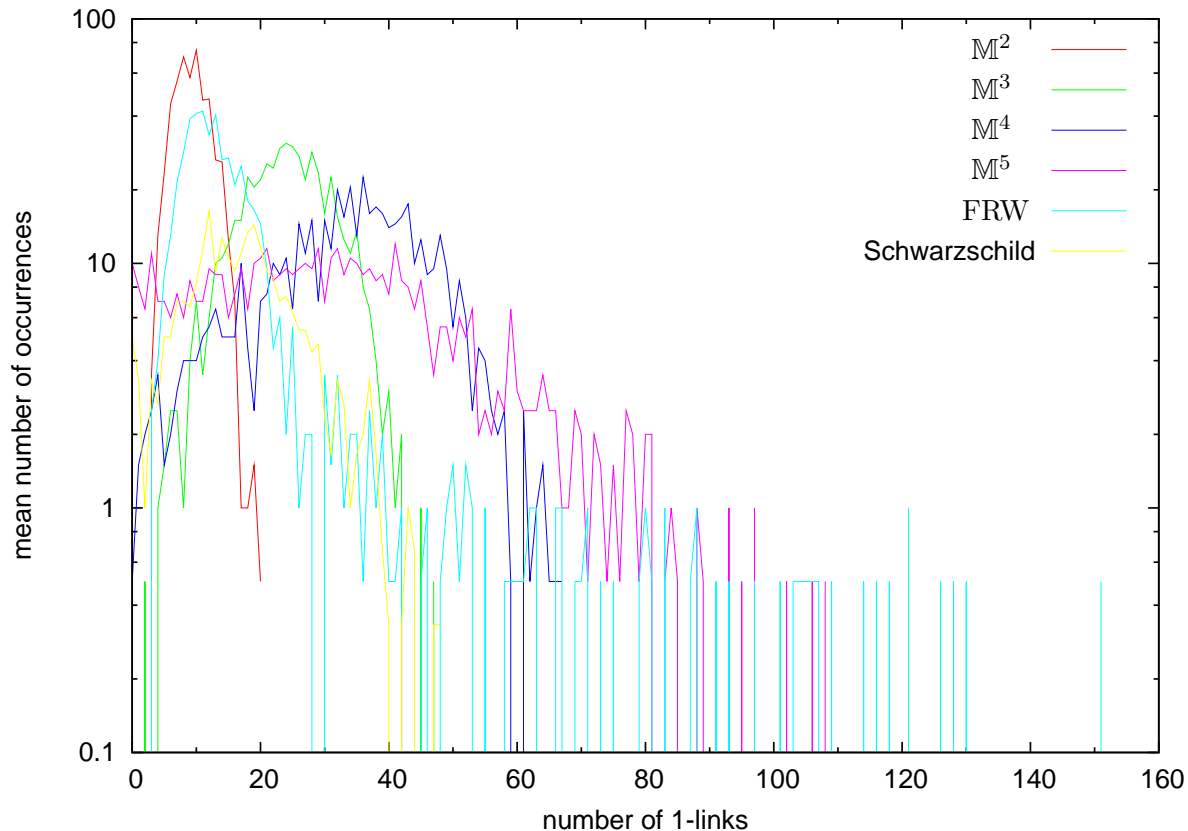


Figure 16. Abundances of (1-)links in some manifoldlike causal sets. Each histogram gives the mean from two sprinklings.

dimensions have the same size (purple), the results closely match that of the interval in \mathbb{M}^4 from figure 17. As the size of the internal dimensions is decreased, the approximately 256 elements of the causal set begin to be unable to ‘see’ the internal dimensions, and the asymptotic behaviour of 2-link counts becomes like those of lower dimensional spacetimes. In the extreme case of the red data, with the ‘internal’ dimensions $\leq \frac{1}{16}$ times the size of the ‘external’, the causal set is not able to resolve the internal dimensions, and the 2-link counts are almost exactly what one finds for an interval in \mathbb{M}^2 . (As an alternative to what we did here, one could instead hold the manifold fixed, and sprinkle increasingly more elements to resolve the small internal dimensions. We chose this approach of varying the manifold at fixed $\langle N \rangle$ simply to save on compute time.)

To see how this works as a measure of manifoldlikeness, we try it on two obviously non-manifoldlike causal sets: the ‘tower of crowns’ and the generic ‘Kleitman-Rothschild orders’. A tower of m -crowns consists of a number of layers (m -antichains). If we label the elements in each layer by $0 \dots m-1$, then element i in layer t precedes elements i and $i+1 \bmod m$ in layer $t-1$. Figure 14 depicts a tower of three 3-crowns. The Kleitman-Rothschild (KR) orders form a generic subset of the set of all finite partially ordered sets [28, 29]. They consist of three layers, the middle of which contains approximately half the elements of the causet set, and the top and bottom layer contain about a quarter each.⁴ For each pair of elements in adjacent layers, we place a relation between them with probability $1/2$. Every element of the bottom

⁴ In our simulations we select the cardinality of the bottom layer from a Poisson distribution with mean $N/4$ (for an N element causet set), and likewise for the top layer. All remaining elements are placed in the middle layer.

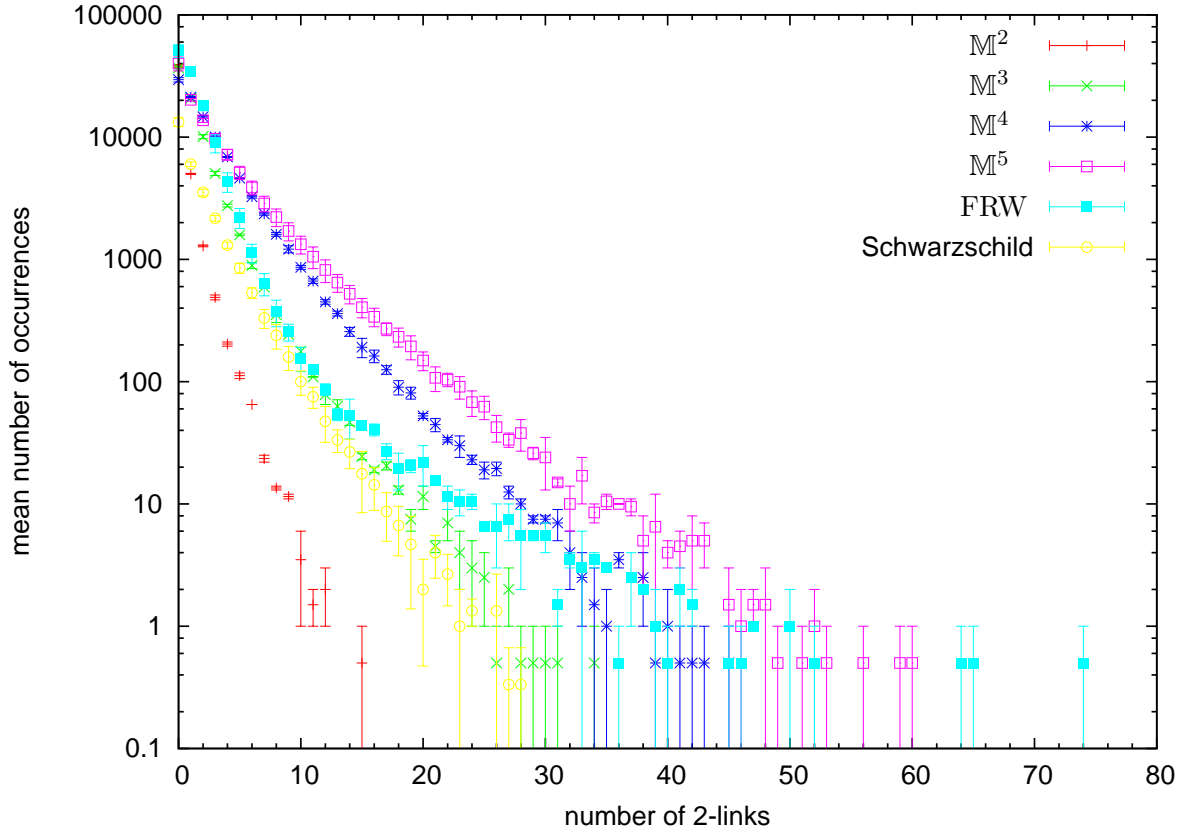


Figure 17. 2-links in some manifoldlike causal sets. Each histogram gives the mean (and standard error) from two sprinklings.

layer precedes every element of the top layer. The results for these causal sets are depicted in figures 19 and 20. The tower of crowns are obviously not manifoldlike, as the only non-zero bins are 2 and 4 for the 1-links, and 0, 1, and 2 for the 2-links. The 1-links histogram for the KR orders looks like it could have come from a sprinkling. The 2-links histogram, however, possess a ‘discontinuity’, with a huge spike at zero followed by empty bins at 1-3. The spike at zero results from unrelated pairs of elements, each from different layers. This sort of behaviour does not resemble sprinklings into spacetime.

The last class of causal sets we consider are those generated by the ‘transitive percolation’ dynamics, which is a simple special case of the generic class of sequential growth models derived in [26]. Here one begins with N elements, and considers every pair of elements $i < j$ in turn, introducing a relation between them with some fixed probability p . After relations are introduced in this way, one takes the transitive closure to arrive at a causal set. In figure 21 we depict the 2-links for two choices of parameters, $N = 2^{15}$, $p = 2/10$, and $N = 128$, $p = 7/10$. They fall off very quickly, but otherwise are not obviously distinct from the results that one gets from sprinkling into spacetime. To get some idea as to whether there are sprinklings into spacetime which mimic these results, we sprinkle into a rectangle of \mathbb{M}^2 , with a height/duration 55 times the (spatial) width. Although the 2-link abundances for transitive percolation at $N = 128$, $p = 7/10$ fall off a bit faster than for the sprinkling into the rectangle, it remains possible that that some choice of parameters for percolation will give a 2-link histogram which can be matched by a sprinkling.

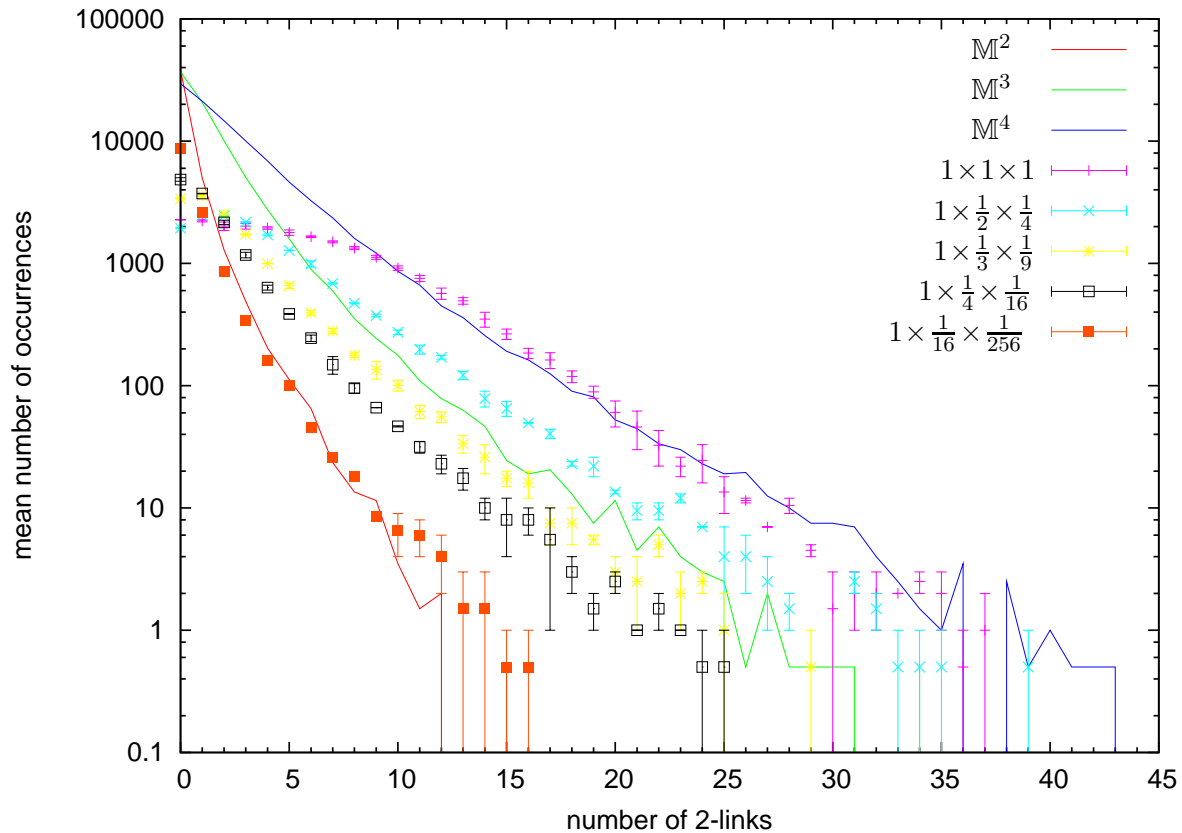


Figure 18. 2-links in $\langle N \rangle = 256$ sprinklings into $T^3 \times I$ spacetimes. The ‘circumferences’ of the toroidal dimensions are given in the key. Each histogram gives the mean (and standard error) from two sprinklings. The solid lines indicate the means from figure 17, for comparison.

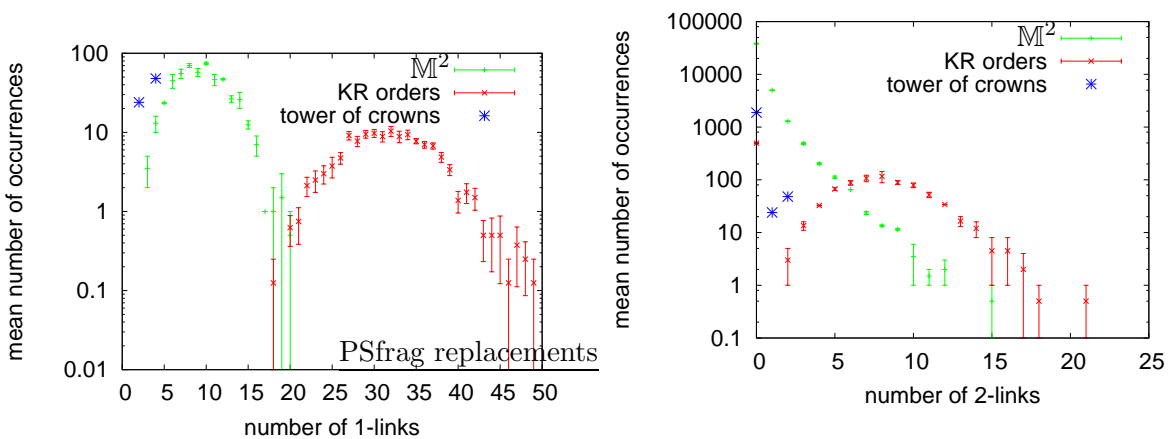


Figure 19. 1-links for some non-manifoldlike causal sets: (Two) Kleitman-Rothschild order(s) on 64 elements, and a tower of 6 12-crowns. Results from sprinkling into \mathbb{M}^2 is added for comparison.

Figure 20. 2-links for some non-manifoldlike causal sets: (Two) Kleitman-Rothschild order(s) on 64 elements, and a tower of 6 12-crowns. Note the large number of pairs in the KR-order (red) without any 2-links. Results from sprinkling into \mathbb{M}^2 is added for comparison.

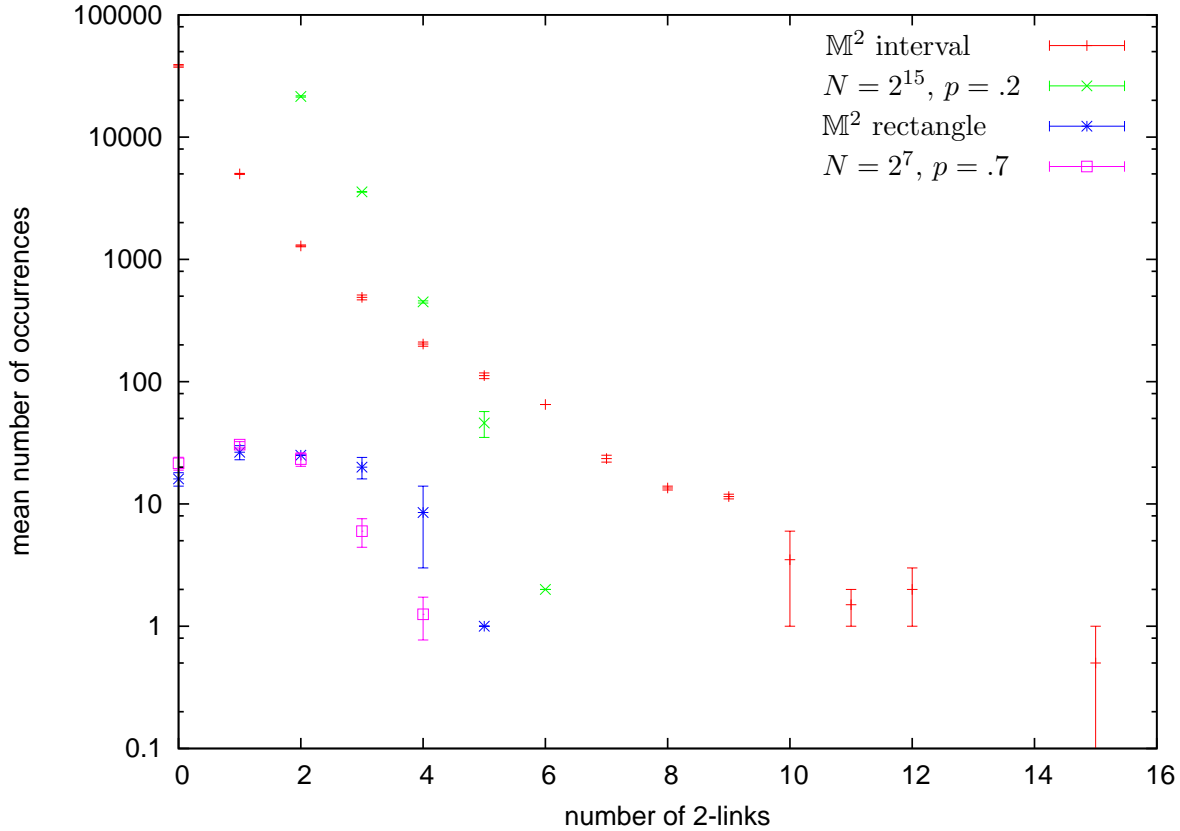


Figure 21. Comparison of transitive percolation with sprinklings into M^2 . The interval in M^2 uses $\langle N \rangle = 512$, while the rectangle $\langle N \rangle = 128$. Each histogram gives the mean and error from two causal sets.

8. Conclusion

A fundamentally atomistic theory of quantum gravity must come with some sort of relation defined on the discrete elements, in order for nontrivial geometric structures to emerge. In the case of causal sets, this relation is regarded as a causal ordering. This association with causality makes it relatively straightforward to see how timelike structures emerge, but spatial quantities are more subtle. Here we proposed some quantities, derived from the discrete causal ordering, which extract spatial information from the causal set, such as spatial distances.

In order to define spatial distance, we introduced the notion of an n -link, which is a simple derived object which encodes information about the intersection of light cones of spatially separated elements. From this we introduced the 2-link distance, and showed that it is able to overcome the degeneracy of the former measure of spatial distance for pairs of elements on a causal set.

In order to recover curved geometry, we further proposed to use the 2-link distance within some local region, to identify spatial nearest neighbors in the causal set. This defines a symmetric, spacelike relation, which is derived from the causal order. From it we may hope to recover the length of continuous curves, and thus derive the metric geometry. It is hoped that such spacetime structures will be useful in the development of a dynamical law for causal sets.

The n -link captures some element of spatial information, which plain links (in and of themselves)

do not. In [22] it was observed that their abundance depends somewhat strongly upon dimension, and it was proposed that they could be used as a dimension estimator, or even as a potentially stringent condition for a causal set to be faithfully embeddable into a spacetime manifold. Here we performed a preliminary investigation of this ‘manifoldlikeness’ condition, and observed somewhat sharp dependence of 2-link abundances on dimension.

In order to see the effect of compact dimensions at various scales, we explored flat $T^3 \times I$ spacetimes, with varying ratios of scales of the ‘internal’ dimensions. We observed that the abundance of 2-links is able to see the correct dimension of 4 at large sprinkling densities, but sees an effective, smaller dimension as the sprinkling density is reduced as compared to the ratio of circumferences of the toroidal dimensions. The results mirror those of [18] for embeddings into $S^1 \times I$ spacetime.

The question of how to compute the dimension of discrete spacetime at a range of length scales is important currently, because of a number of results from various approaches to quantum gravity which predict a scale dependent dimension, in particular a smaller fractal dimension at high energies [30] (and references therein). In addition to the older methods mentioned in the introduction, counting of n -links may provide an important alternate method to deduce which dimensions arise dynamically at various scales in causal set quantum gravity.

In section 7 we presented some preliminary results on a manifoldness test based on counting n -links. It is easily able to distinguish some obviously non-manifoldlike causal sets from those which are faithfully embeddable into spacetime, however it had some difficulty in distinguishing causal sets generated from transitive percolation from those of sprinklings into regions of Minkowski space. This may be rectified when considering n -links for $n > 2$, or by performing a careful analysis on the parameter space of the transitive percolation and sprinkling models. Of course it can only be a necessary condition for there to exist a faithful embedding into spacetime, and not sufficient, because one can always compose partial orders with a particular form for the n -link counts, which is not manifoldlike.

Acknowledgments

This research was supported primarily by the Perimeter Institute for Theoretical Physics. Research at Perimeter Institute is supported by the Government of Canada through Industry Canada and by the Province of Ontario through the Ministry of Research & Innovation. Earlier work was supported by the Marie Curie Research and Training Network ENRAGE (MRTN-CT-2004-005616), and the Royal Society International Joint Project 2006-R2. Some numerical results were made possible by the facilities of the Shared Hierarchical Academic Research Computing Network (SHARCNET:www.sharcnet.ca).

References

- [1] Thiemann T 2007 *Modern Canonical Quantum General Relativity* (Cambridge University Press)
- [2] Ashtekar A 2004 *Class.Quant.Grav.* **21** R53 (*Preprint gr-qc/0404018*)
- [3] Rovelli C 2004 *Quantum Gravity* (Cambridge University Press)
- [4] Konopka T, Markopoulou F and Severini S 2008 *Phys. Rev.* **D77** 104029 (*Preprint 0801.0861 [hep-th]*)
- [5] Wolfram S 2002 *A New Kind of Science* (Wolfram Media, Inc.)
- [6] Hama A, Markopoulou F, Premont-Schwarz I and Severini S 2009 *Phys. Rev. Lett.* **102** 017204 (*Preprint 0808.2495 [quant-ph]*)
- [7] Rideout D and Zohren S 2006 *Class.Quant.Grav.* **23** 6195–6213 (*Preprint gr-qc/0606065*)
- [8] Bombelli L, Lee J, Meyer D and Sorkin R D 1987 *Phys. Rev. Lett.* **59** 521–524
- [9] Sorkin R D 1994 *Modern Physics Letters A* **9** 3119–3127 (*Preprint gr-qc/9401003*)
- [10] Sorkin R D 2007 *J. Phys. A: Math. Gen.* Special Issue: Quantum Universe, [quant-ph/0610204](#)
- [11] Craig D and Hartle J B 2004 *Phys. Rev.* **D69** 123525 (*Preprint gr-qc/0309117*)
- [12] Noldus J 2004 *Class.Quant.Grav.* **21** 839–850
- [13] Malament D B 1977 *J. Mathematical Phys.* **18** 1399–1404

- [14] SW Hawking AR King P M 1976 *J. Math. Phys.* **17** 174–181
- [15] Sorkin R D 2005 *Lectures on Quantum Gravity, Proceedings of the Valdivia Summer School, Valdivia, Chile, January 2002* ed Gomberoff A and Marolf D (Plenum) (*Preprint gr-qc/0309009*)
- [16] Reid D D 2003 *Phys. Rev. D* 024034 [gr-qc/0207103](#)
- [17] Myrheim J 1978 CERN preprint TH-2538
- [18] Meyer D A 1988 *The Dimension of Causal Sets* Ph.D. thesis Massachusetts Institute of Technology
- [19] Bachmat E 2008 *Contemporary Mathematics* **458** 347–359 (*Preprint gr-qc/0702140*)
- [20] Henson J 2007 *Towards Quantum Gravity* ed Oriti D (Cambridge University Press) (*Preprint gr-qc/0601121*)
- [21] Brightwell G and Gregory R 1991 *Phys. Rev. Lett.* **66** 260–263
- [22] Rideout D and Wallden P 2008 *Preprint 0810.1768* [[gr-qc](#)]
- [23] Goodale T, Allen G, Lanfermann G, Massó J, Radke T, Seidel E and Shalf J 2003 *Vector and Parallel Processing — VECPAR 2002, 5th International Conference* (Berlin: Springer) pp 197–227
- [24] Major S, Rideout D and Surya S 2009 *Preprint 0902.0434* [[gr-qc](#)]
- [25] Sorkin R D 2007 *Towards Quantum Gravity* ed Oriti D (Cambridge University Press) (*Preprint gr-qc/0703099*)
- [26] Rideout D P and Sorkin R D 2000 *Phys. Rev. D* **61** 024002 (*Preprint gr-qc/9904062*)
- [27] He S and Rideout D 2008 *Preprint 0811.4235* [[gr-qc](#)]
- [28] Brightwell G 1993 *Surveys in Combinatorics (London Math. Soc. Lecture Notes Series vol 187)* ed Keith pp 53–83
- [29] Kleitman D and Rothschild B 1975 *Trans. Amer. Math. Society* **205** 205–220
- [30] Modesto L 2008 *Preprint 0812.2214* [[gr-qc](#)]